

Electronic Supplementary Information (ESI)

Large-scale fabrication of hierarchical α -Fe₂O₃ assemblies as high performance anode materials for lithium-ion batteries

Ruguang Ma,^a Lifang He,^a Zhouguang Lu,^{*b} Shiliu Yang,^a Liujiang Xi,^a and Jonathan C. Y. Chung^{*a}

^a *Department of Physics and Materials Science, City University of Hong Kong, 83 Tat Chee Avenue, Kowloon, Hong Kong, China. Fax: +852 3442 0538; Tel: +852 3442 7835; E-mail: appchung@cityu.edu.hk*

^b *Department of Micro-Nano Materials and Devices, South University of Science and Technology of China, Shenzhen, Guangdong 518055, China. E-mail: luzg@sustc.edu.cn*

10

15

20

25

30

35

40

Experimental Section

Synthesis

In a typical procedure for preparing flower-like α - $\text{FeF}_3 \cdot 3\text{H}_2\text{O}$ microparticles, 8.11g of iron (III) chloride (FeCl_3 , Sigma-Aldrich, $\geq 98\%$) was dissolved in 10 mL of deionized water to form a clear yellowish solution which was then poured into HF solution (48%, 20mL) under magnetic stirring at room temperature (RT). (Note that HF solution is highly corrosive and must be manipulated very carefully.) A large amount of white precipitates formed instantly after 10 mL absolute ethanol was introduced into the mixture solution. β - $\text{FeF}_3 \cdot 3\text{H}_2\text{O}$ was prepared by a similar procedure except that the FeCl_3 powders were dissolved in ethylene glycol (EG) instead of water. The precipitates (powders) were washed with ethanol and deionized water for several times. After centrifugation, the powders were dried at 60 °C overnight in a vacuum oven. Then the powders were heat-treated at 600 °C for 4h in a tube furnace under a continuous high-purity nitrogen gas flow. The product obtained from the white powder (α - $\text{FeF}_3 \cdot 3\text{H}_2\text{O}$) was marked as “flower-like Fe_2O_3 ” while the pink powder (β - $\text{FeF}_3 \cdot 3\text{H}_2\text{O}$) was denoted as “cubic Fe_2O_3 ”.

For the sake of comparison, normal Fe_2O_3 nanoparticles with the size of ~ 150 nm (labeled as “150 nm Fe_2O_3 ”) were synthesized according to literature ¹. Typically, 2 mmol of FeCl_3 was dissolved into 80 mL of distilled water to form a transparent solution followed by adding 6 mmol of KCl to the solution. After stirring for 30 min, the obtained solution was transferred and sealed into a 100 mL Teflon -lined autoclave, heated at 180 °C for 12 h, and then cooled to RT naturally. The as-prepared precipitate was washed several times with distilled water, collected by centrifuging, and finally dried at 60 °C in vacuum.

Characterization

X-ray diffraction (XRD) patterns in the 2θ range of 10-80° were obtained by employing a Siemens D500 diffractometer with Cu K_α radiation at a scan rate of $0.02^\circ \text{ s}^{-1}$. The morphology of the precursor and α - Fe_2O_3 was examined with scanning electron microscope (SEM, JEOL-820) and a Philips XL30 FEG field-emission SEM (FESEM). To understand the evolution of the powders from precursors to α - Fe_2O_3 , thermal gravimetric (TG, Q50) analysis was employed from RT to 650 °C under a nitrogen ventilation of 40 mL min^{-1} at a heating rate of $5^\circ \text{ C min}^{-1}$. Ex situ XRD measurements were immediately performed and completed within 5 min after the powder of precursor was annealed under nitrogen atmosphere at designated temperatures for 1h. In order to observe the morphology of the

intermediate during the conversion from the precursor to α -Fe₂O₃, the powder was annealed at a given temperature for 1h under N₂ atmosphere. Then the intermediate was sealed into a small bottle in an Ar-filled glovebox. Before observing the intermediate, the small bottle was reopened and the intermediate was put inside the SEM chamber, thereby minimizing the exposure to atmosphere within one minute. Transmission electron microscopy (TEM) and high-resolution TEM (HRTEM) images were obtained from the equipment of CM200 FEG operated at 200kV. Samples for TEM were ultrasonically dispersed in 10 mL of ethanol for 30min before putting on a carbon grid supported by a copper grid. The specific surface areas of the three α -Fe₂O₃ samples were analyzed by nitrogen (N₂) adsorption/desorption isotherms at 77 K using a NOVA 1200e Surface Area and Pore Size Analyzer (Quantachrome Instruments). Prior to adsorption experiments, the samples were outgassed in vacuum at 150 °C for 2h.

10 **Electrochemical Characterization**

Electrochemical characterization was performed in the form of CR2032 coin-type lithium half cells. The slurry was prepared by mixing the active material (α -Fe₂O₃), acetylene black and polyvinylidene fluoride (PVDF) with a weight ratio of 8:1:1 in 1-methyl-2-pyrrolidinone (NMP) solvent. The blended slurry was then cast onto a Cu foil current collector and dried at 200 °C for 10 h in a tube furnace under a nitrogen atmosphere.² The cell was assembled in an Ar-filled glovebox using lithium foil as counter electrode, one layer of Celgard 2032 (Celgard, Inc., USA) as the separator, and 1 M LiPF₆ dissolved in ethylene carbonate (EC) and dimethyl carbonate (DMC) (1:1 in volume) as the electrolyte. Both cyclic voltammetry (CV) and impedance measurements were performed on a Zahner IM6 electrochemical workstation. CV curves were recorded at RT between 0.01 and 3 V (vs. Li⁺/Li) at a scan rate of 0.1 mV s⁻¹. Galvanostatic discharge-charge experiments were carried out at RT with an Arbin Instruments (BT200, College Station, TX) system. The cells were cycled between 0.01~3 V (vs. Li⁺/Li) at different current densities for rate performance and at 200mAhg⁻¹ (~0.2 C) for cycling performance. (1 C rate corresponds to the current density of 1007 mA g⁻¹.) Electrochemical impedance spectra (EIS) were obtained after a 2 h rest by applying an ac voltage of 2.5 mV amplitude over the frequency range 100 k Hz to 10 m Hz at different stages, such as after the initial discharge and the 100th cycle. The EIS parameters were simulated by ZSIMPWIN software.

25

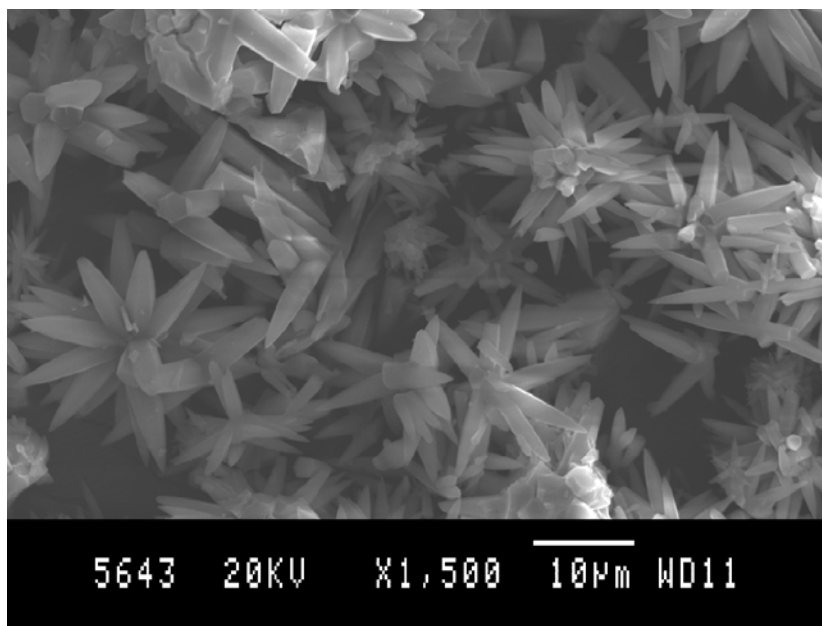


Fig. S1 An overview SEM image of the flower-like $\alpha\text{-FeF}_3\cdot 3\text{H}_2\text{O}$.

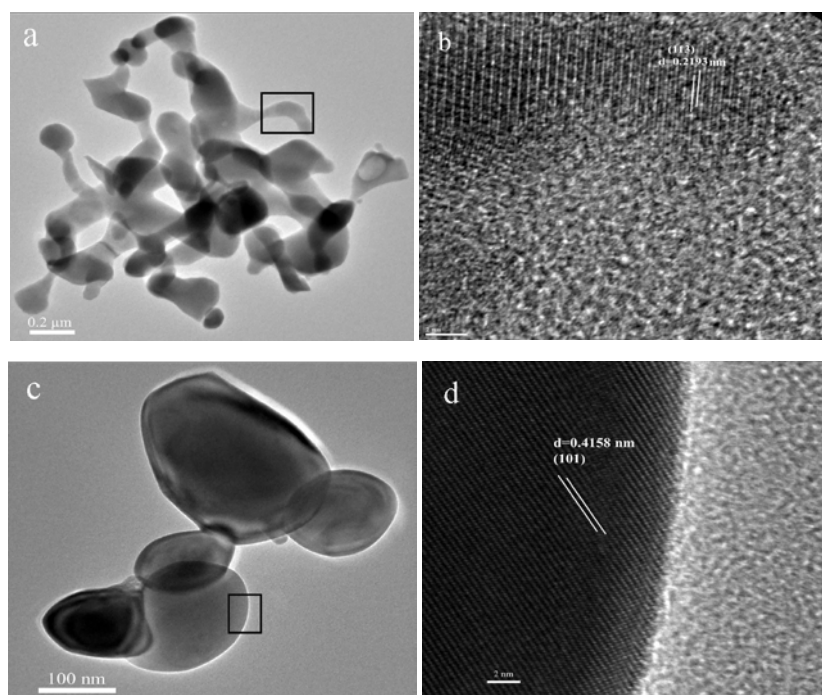


Fig. S2 (a) TEM and (b) HRTEM images of the flower-like $\alpha\text{-Fe}_2\text{O}_3$ produced from $\alpha\text{-FeF}_3\cdot 3\text{H}_2\text{O}$. (c) TEM and (d) HRTEM images of cubic $\alpha\text{-Fe}_2\text{O}_3$ produced from $\beta\text{-FeF}_3\cdot 3\text{H}_2\text{O}$

TEM images as demonstrated in Fig. S2 provide more insight into the microstructure of the hierarchical porous $\alpha\text{-Fe}_2\text{O}_3$ powders. It indicates that the $\alpha\text{-Fe}_2\text{O}_3$ powders produced from both $\alpha\text{-FeF}_3\cdot 3\text{H}_2\text{O}$ and $\beta\text{-FeF}_3\cdot 3\text{H}_2\text{O}$ are composed of interconnected nanoparticles with a size of $\sim 150\text{nm}$. This kind of netlike structure could contribute to an improvement in the electron transport due to low resistance of the related electrode³ and is expected to enhance the cyclability. Fig. S2b & d show the HRTEM images from the areas marked by black panes in Fig. S2a & c,

respectively. The clear lattice fringes with the spacing of 0.219 and 0.416 nm can be indexed to the planes of (113) and (101) of α -Fe₂O₃, respectively, indicating good crystallinity of the produced α -Fe₂O₃.

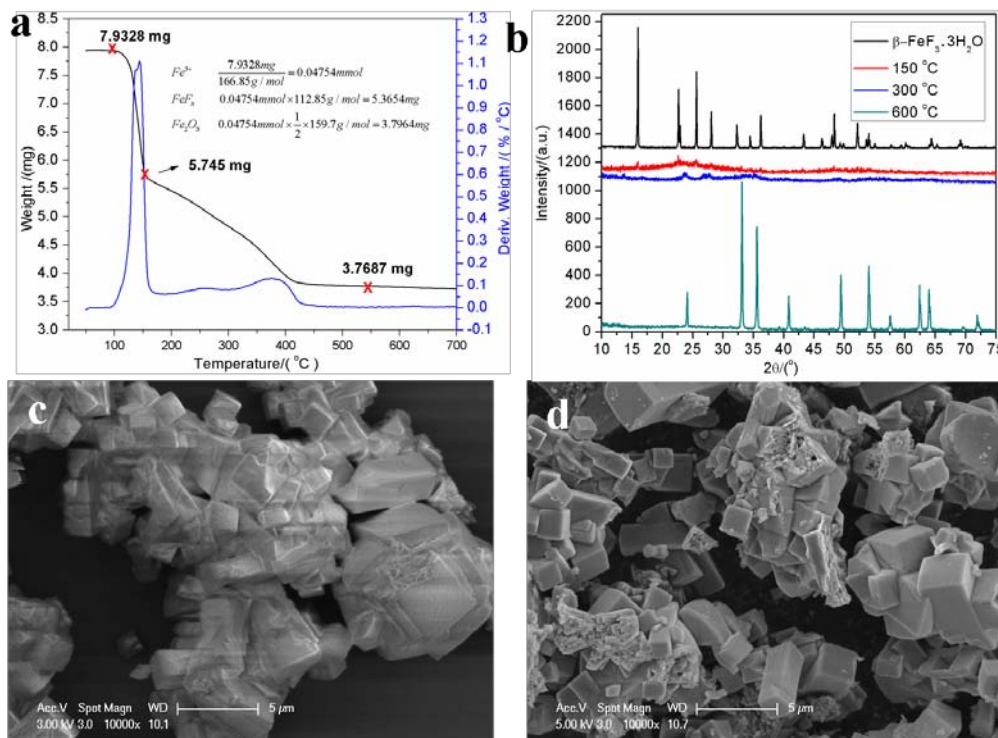


Fig. S3 (a) TGA curve of the β -FeF₃·3H₂O under nitrogen atmosphere. (b) Ex situ XRD patterns of the cubic shaped β -FeF₃·3H₂O calcined at different temperatures for 1h. (c) SEM image of the cubic β -FeF₃·3H₂O calcined at 150 °C for 1h. (d) SEM image of the cubic β -FeF₃·3H₂O calcined at 300 °C for 1h.

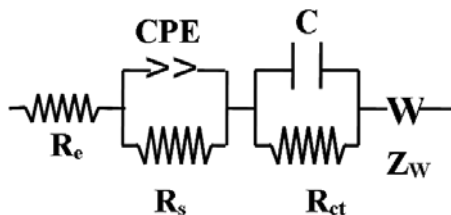


Fig. S4 equivalent electrical circuit used for simulating the EIS data.

In the electrochemical impedance spectrum, the first semicircle in the high frequency region represents the resistance (R_s) paralleled with the capacitance (C), which is related to Li-ion migration through multilayer surface films (including SEI layer and surface modification layer), while the intercept at the Z' axis corresponds to the ohmic resistance of working electrode (R_Ω). The second semicircle at lower frequency correlates to the insertion/extraction process of Li-ion, corresponding to the charge transfer resistance (R_{ct}) and a constant phase element (CPE_{ct}) at interface.⁴ The inclined line at low frequency region represents the Warburg impedance (Z_w), which is associated with Li-ion diffusion in the particles.⁵

Table S1 The simulated electrochemical impedance parameters of the three electrodes after the initial discharge.

| | R_{Ω} (Ω) | R_s (Ω) | R_{ct} (Ω) |
|-----------------------|---------------------------|--------------------|-----------------------|
| Flower-like Fe_2O_3 | 4.70 | 179 | 96.7 |
| Cubic Fe_2O_3 | 4.78 | 130.5 | 92 |
| 150nm Fe_2O_3 | 4.62 | 225.1 | 115.4 |

^a Footnote text.

Table S2 The simulated electrochemical impedance parameters of the three electrodes after the 100th cycle.

| | R_{Ω} (Ω) | R_s (Ω) | R_{ct} (Ω) |
|-----------------------|---------------------------|--------------------|-----------------------|
| Flower-like Fe_2O_3 | 33.5 | 145.6 | 15.8 |
| Cubic Fe_2O_3 | 30.5 | 125 | 12.1 |
| 150 nm Fe_2O_3 | 26.3 | 196 | 21.2 |

^s Footnote text.

References

1. X. L. Wu, Y.-G. Guo, L.-J. Wan and C.-W. Hu, *J. Phys. Chem. C*, 2008, **112**, 16824.
2. J. Li, H. M. Dahn, L. J. Krause, D. B. Le and J. R. Dahn, *J. Electrochem. Soc.*, 2008, **155**, A812;
- 10 3. W. Zhou, L. Lin, W. Wang, L. Zhang, Q. Wu, J. Li and L. Guo, *J. Phys. Chem. C*, 2011, **115**, 7126.
4. M. V. Reddy, T. Yu, C.-H. Sow, Z. X. Shen, C. T. Lim, G. V. S. Rao and B. V. R. Chowdari, *Adv.Func. Mater.*, 2007, **17**, 2792.
5. M. D. Levi and D. Aurbach, *J. Phys.I Chem. B*, 2004, **108**, 11693.

15